

Cyclic Softening Modeling with the Distribution of Non Linear Relaxation (Dnlr) Approach

L. Dieng¹ , A. Abdul-Latif² , M. Haboussi and C. Cunat³

Abstract: Being of particular interest in this work, a complicated phenomenon related to cyclic softening of metallic polycrystals is modeled. As in the Waspaloy, this phenomenon can take place when a non-proportional tension-torsion cyclic loading of 90° out-of-phase is followed, after cyclic steady state, by a uniaxial one (tension-compression) with the same maximum equivalent plastic strain. By using the DNLR (Distribution of Non Linear Relaxation) model recently proposed by the authors describing the cyclic plasticity of metals, a new extension is here developed. It is recognized that such an extension can satisfactorily reproduce this softening phenomenon. It is noteworthy that this model describes such a phenomenon with a minimum number of material parameters in comparison with other phenomenological models. After calibration of the model parameters for the Waspaloy, the constitutive equations of the model are then implemented in a commercial finite element code to simulate the model response vis-à-vis a given structure made from the Waspaloy. Finally, it is found that the new extension as well as the finite element predictions give a fairly well accordance with the available experimental results.

Keyword: DNLR, Cyclic Plasticity, Relaxation, Complex Loading, Cyclic Softening, Finite Element Predictions.

1 Introduction

When mechanical structural components are subjected to complex loading situations, it has been shown that the cyclic deformation behavior for

metallic materials are highly sensitive to the type of these in-phase or out-of-phase loading paths [Abdul-Latif, Clavel, Ferney, and Saanouni (1994); Abdul-Latif (1996); Benallal and Marquis (1987); Blackmon, Socie, and Leckie (1983); Clavel, Pilvin, and Rahouadj (1989); Doong and Socie (1991); Fatemi and Kurath (1988); Kanazawa, Miller, and Brown (1977); Lamba and Siddebottom (1978a); Lamba and Siddebottom (1978b); McDowell (1985) and many others]. This seems to be due to distinct important features related to metallurgical changes at highly stressed or strained regions affected generally by the applied cyclic loading conditions.

The DNLR model [Cunat (2001); Dieng (2002); Dieng, Abdul-Latif, Haboussi, and Cunat (2005); Dieng, Haboussi, Loukil, and Cunat (2005); Loukil (1996)] based on the generalization of the Gibbs's relation [Gibbs (1970)] away from the equilibrium for a spatially uniform system is used. It adopts also the fluctuation theory to analyze the material dissipation due to its internal reorganizations. In this approach, it is assumed that the local behavior within the representative volume element (RVE) is determined by a thermodynamic potential, which contains all the necessary informations about the system. The incremental constitutive equations are directly obtained from the knowledge of the second order derivatives of the non equilibrium potential function (generalized Tisza's matrix coefficients) completed by kinetic modeling of internal reorganizations. In order to treat a continuous medium, the definition of a local potential is adopted. Taking into consideration the exchange among different RVEs, this allows to construct a theory of the fields where one finds probably its limit when the local gradients on the intensive values become highly important. In such a case, the volume element be-

¹ LCPC, Nantes, France.

² IUT de Tremblay, France.

³ LEMTA, Nancy University, CNRS, France.

havior can be appropriately represented by an averaging intensive value. Moreover, another characteristic of the DNLR approach is the spectral analysis of dissipation phenomena related to microstructural internal reorganizations where it is assumed that the departure from equilibrium can be analyzed as a function of the former equilibrium state and the kinetics of the relaxation phenomena like in chemical reactions [Cunat (2001)]. An excess term of energy (or entropy) plays a role of composition adaptation in order to establish a partial equilibrium or a constrained equilibrium. The obtained deviation from the equilibrium corresponds to the fluctuation used in this approach. For practical reason, the specificity of the DNLR is to consider a modal representation, which is based on the introduction of a quasi-infinite number of dissipative modes using only two adjustable parameters for describing the corresponding initial relaxation spectrum by means of fluctuation theory. The complex return to equilibrium is depicted by a spectral analysis in which normal dissipative modes are able to reproduce the whole phenomenon of relaxation. Consequently, the kinetic law of each individual mode is described as a first order non-linear one and developed in the framework of the activated state theory.

From a modeling standpoint, the constitutive equations already proposed by many research programs for reproducing the uniaxial cyclic behavior are generally capable to correlate successfully the experimental results. Nevertheless, modeling of multiaxial deformation features becomes a difficult task due to the complexity of the material response under non-proportional loading paths. In other words, high cyclic non-proportionality leads to a high hardening (isotropic and/or kinematic) behavior complexity due to the effects of the change in plastic strain rate direction. It is well known that this change in direction has a primordial role in inducing extra slip systems activation for several metallic materials. Many cyclic plasticity and viscoplasticity models have therefore a complex mathematical form and posses, in general, a large number of material constants which need a wide experimental database to be identified. The DNLR approach gives, at least, a partial

solution for such modeling difficulties, i.e., it does not use any internal state variables for the plastic strain and hardening (isotropic and/or kinematic) and has relatively low model parameters.

Recently, the DNLR formalism has been developed in the objective to reproduce the cyclic behavior of metallic materials under various simple and complex loading paths [Dieng, Haboussi, Loukil, and Cunat (2005)] without damage. Its capability to reproduce several phenomena such as: Bauschinger and strain memory effects, additional hardening, etc, was appropriately illustrated. As far as the ratcheting phenomenon is concerned, a not yet published work of the authors confirms that the model shows again its powerful to describe this cyclic phenomenon. The originality of such a model is related to its capability to reproduce the principal mechanical cyclic phenomena under simple and complex loading conditions with relatively few model parameters (8 adjustable parameters and 2 parameters of elasticity). Though, other approaches use with this intention a score of 20 coefficients (for example, Abdul-Latif, Clavel, Ferney, and Saanouni (1994); Abdul-Latif (1996); Benallal and Marquis (1987)).

In this work, the cyclic softening phenomenon observed in the Waspaloy case [Clavel, Pilvin, and Rahouadj (1989)], which cannot be described by the model presented in [Dieng, Abdul-Latif, Haboussi, and Cunat (2005)], is modeled. As a matter of fact, this phenomenon is experimentally observed when a non-proportional cyclic loading of 90° out-of-phase is applied up to stabilization, then followed by a uniaxial cyclic loading of tension-compression, with the same equivalent maximum plastic deformation. In the first phase of non-proportional loading, a phenomenon of additional hardening is obviously recorded during which an activated slip systems multiplicity occurs. On the other hand, an evanescent hardening is observed during the second phase of uniaxial loading. This is undoubtedly related to decreasing of the slip systems multiplicity [Clavel, Pilvin, and Rahouadj (1989)]. Thus, a special emphasis is placed on an extension of the DNLR model developed in [Dieng, Abdul-Latif, Haboussi, and

Cunat (2005)] so as to describe this complicated phenomenon correctly. A finite element implementation of the model is then realized so as to assess the capability of such modeling to reproduce the softening effects at the structural scale. After the implementation of the model equations in a commercial finite element code, the recorded prediction for a given structure made from the Was-paloy reveals a fairly well accordance with the experiments.

The present work consists of two essential parts, the first one deals with the material modeling aspect, i.e., model constitutive equations. After the identification of the model constants for the Was-paloy, a quantitative study is carried out in the second part of this study.

2 Presentation of the DNLR formalism

2.1 General statement

The Distribution of Non Linear Relaxations (DNLR) formalism initially introduced by Cunat (2001), is based on the thermodynamic of the irreversible processes and the theory of the fluctuation. In this formalism, the existence of a generalized thermodynamic potential (Ψ) is postulated. It is obtained by Legendre transform of the internal energy according to selected experimental loading paths. It contains all the information of the system including that for those situations away from equilibrium. This postulate constitutes, in fact, a double generalization of the fundamental Gibbs's relation [Gibbs (1970)] for systems out-of-equilibrium, in the sense that (i) it is admitted that the potential preserves its status (of potential) out-of-equilibrium in accordance with the thermodynamic of De Donder (1920), (ii) the entropy remains to define the out-of-equilibrium situation of the system, and the temperature is its dual variable. The latter recovers its usual significance in equilibrium. Hence, starting from the potential $\Psi = \Psi(\underline{\gamma}, \bar{z})$, it is possible to write the following equations describing the evolution of the system out-of-equilibrium for a given RVE:

$$\begin{pmatrix} \dot{\underline{\gamma}} \\ -\dot{\bar{A}} \end{pmatrix} = \begin{pmatrix} \underline{\underline{a}}^u & \bar{b} \\ \bar{b} & \bar{\bar{g}} \end{pmatrix} \begin{pmatrix} \dot{\underline{\gamma}} \\ \dot{\bar{z}} \end{pmatrix} \quad (1)$$

where $\underline{\gamma}$ represents the perturbation imposed on the system (observable variables on the RVE), β the corresponding response. The internal variable \bar{z} and the affinity variable \bar{A} describe the internal reorganization of the system and the induced dissipation. The following matrices connect these dual variables:

$$\begin{aligned} \underline{\underline{a}}^u &= \frac{\partial^2 \Psi}{\partial \underline{\gamma} \partial \underline{\gamma}} (\underline{\gamma}, \bar{z}), & \bar{b} &= \frac{\partial^2 \Psi}{\partial \underline{\gamma} \partial \bar{z}} (\underline{\gamma}, \bar{z}) \\ \text{and } \bar{\bar{g}} &= \frac{\partial^2 \Psi}{\partial \bar{z} \partial \bar{z}} (\underline{\gamma}, \bar{z}) \end{aligned} \quad (2)$$

When the coefficients of these coupling matrices are constant, one finds the traditional description of the quadratic potential which leads to the linear models (generalized Zener or Poynting-Thomson model [Poynting and Thomson (1902)]). Note that close to equilibrium, the affinity \bar{A} and the flux variable \bar{z} are linearly dependent through the constant matrix \bar{L} of Onsager. To define this kinetic in the presence of non-linearity, the Onsager relation is generalized as:

$$\bar{z} = \bar{\bar{L}}(z) \bar{A} \quad (3)$$

$\bar{\bar{L}}$ depends *a priori* on z . Moreover, by taking into consideration the relaxed state ($\bar{A}^r = 0$ and $\bar{z} = \bar{z}^r$) the De Donder's relation [DeDonder (1920)] lays down a proportionality rule between the affinity \bar{A} and the internal variables ($\bar{z} - \bar{z}^r$) via the coupling matrix $\bar{\bar{g}}$ given by:

$$\bar{A} = -\bar{\bar{g}}(\bar{z} - \bar{z}^r) \quad (4)$$

The intrinsic dissipation of the affinity \bar{A} and the flux variable \bar{z} should be positive according to the second law of thermodynamic $\bar{A}\bar{z} > 0$, which leads to the definition of relaxation time matrix:

$$\bar{\tau}^{-1} = \bar{\bar{L}}\bar{\bar{g}} \quad (5)$$

By diagonalizing this relaxation time matrix according to Meixner (1949), one can deduce the following expression from equations (3) to (5) :

$$\dot{z}^j = -\frac{z^j - z^{j,r}}{\tau^j} \quad (6)$$

where τ^j is the j eigenvalue of $\bar{\tau}$ corresponding to the dissipation mode j . Afterward, an analysis of

the dissipation modes distribution is proposed in the linear and nonlinear cases. For each mode, the relaxation time τ^j will be defined and its contribution to the overall material response, symbolized hereafter by p_0^j , will be clarified as well as the relation between p_0^j and τ^j determining the relaxation spectrum.

2.2 Distribution of the dissipation modes: linear kinetics case

The relaxation times of the dissipation modes are linearly determined for a RVE close to equilibrium. Indeed, when the RVE is submitted to a perturbation γ , it reacts by an instantaneous response affecting moderately the entropy configuration. Internally, the system is then not in equilibrium and its state can be regarded as a fluctuation around the equilibrium state. In this work, the description of the return to a new equilibrium state (fluctuation regression) according to the activated transitory state theory of Eyring (1936) is adopted. Therefore, the relaxation time for the mode j of regression is defined as follows:

$$\tau^{j,r} = \mu \exp \left(\frac{\Delta F^{j,r}}{RT} \right) \quad (7)$$

where μ is an atomic reference frequency for local jumps which can be approximated by the term $(h/k_B T)$ (h is the Planck constant, k_B the Boltzmann constant, T the temperature and R the ideal gas constant). In spite of such a theoretical limitation, this approximation is resolved, at least partially, by the adjusting of the free energy parameter.

$\Delta F^{j,r}$ is the Helmholtz's free activation energy for the j mode at the relaxed state for the initial position of the activation col (FIG. 1). Such a col corresponds to a metastable equilibrium state and indicates the magnitude of the energy barrier which should be crossed by the material system to reach a new stable equilibrium state.

To evaluate the weight p_0^j on the overall reponse of each dissipative mode, Cunat (2001) used the equipartition principle of the entropy of Prigogine (1968). Consequently, the relation between the j mode weight p_0^j and its corresponding relaxation

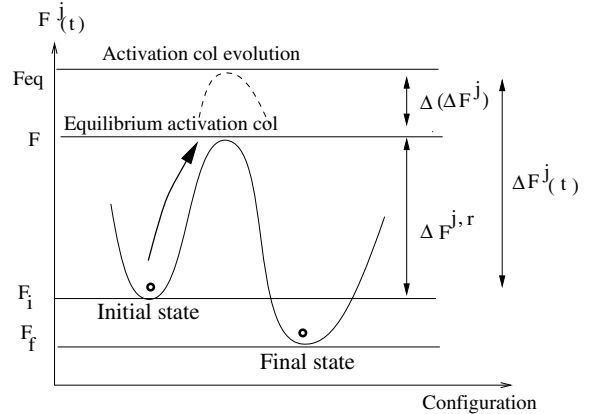


Figure 1: Activation col evolution

time is given by:

$$p_0^j = B \sqrt{\tau^{j,r}} \quad \text{and} \quad \sum_{j=1}^N p_0^j = 1 \quad (8)$$

$$\text{with} \quad \frac{1}{B} = \sum_{j=1}^N \sqrt{\tau^{j,r}}$$

where N represents the number of modes. Equations (8) permit to define the initial distribution spectrum of the dissipation modes (see FIG. 2) and to describe the response generated by the loading condition. Numerically, the chosen continuous spectrum ($N \rightarrow \infty$) is replaced by a discretized one, where N is taken equal to 50 over $D=6$ decades of time scale (this adopted value is justified by the fact that the model response is no longer sensitive to the of D when the latter exceeds 6). The activation energies used in this discretization correspond to:

$$\Delta F^{j,r} = \Delta F_{max}^r - RT \frac{D(N-j)}{N-1} \ln(10)$$

$$\text{for which} \quad 10^{-6} \leq \frac{\tau^{j,r}}{\tau^{r,max}} \leq 1 \quad (9)$$

According to (9), ΔF_{max}^r , which represents the relaxation time of the slowest mode of dissipation, is thus sufficient, as the spectrum width D is fixed, to approximate a continuous distribution of characteristic times with $N = 50$.

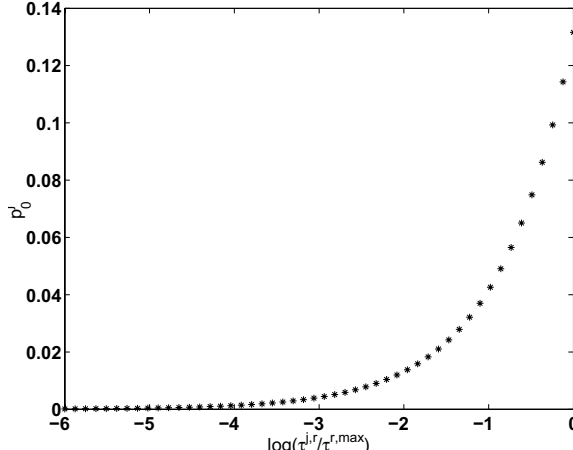


Figure 2: Initial distribution of relaxation times

2.3 Nonlinear kinetics extension

To generalize the description of those situations away from equilibrium, the relaxation times are modified with the aim of taking into account the temporal nonlinearities due to coupling phenomena. The j -relaxation time is obtained from the activated transitory state theory of Eyring (1936) adopted for our problem:

$$\begin{aligned} \tau^j &= \mu \exp \left[\frac{\Delta F^{j,r} + \Delta(\Delta F^j)}{RT} \right] \\ &= \tau^{j,r} \exp \left[\frac{\Delta(\Delta F^j)}{RT} \right] \end{aligned} \quad (10)$$

$\Delta(\Delta F^j)$ represents the variation of the free energy of activation corresponding to the activation col evolution due to the non linearity effects (FIG. 1). Besides, it is assumed that $\Delta(\Delta F^j)$ is the same for the whole modes (cooperative effect) and will be given for the mechanical problem by:

$$\Delta(\Delta F^+) = K_\sigma J_2(\underline{\sigma} - \underline{\sigma}^r) \quad (11)$$

where $K_\sigma = -V^+(cm^3/mol.at.)$ is the average activation volume parameter and $J_2(\underline{\sigma})$ is the equivalent von-Mises stress. The considered nonlinearity corresponds to the memory effects of the second order. Combined to the first order one, the latter permits to describe phenomena such as the distortion of yield surfaces [Loukil (1996); Dieng, Haboussi, Loukil, and Cunat (2005)] or

the cyclic hardening behavior of metallic materials under non-proportional loading paths [Dieng, Abdul-Latif, Haboussi, and Cunat (2005)].

2.4 Mechanical behavior

For purely mechanical problems, the perturbation γ corresponds to the strain $\underline{\varepsilon}$ and the response β to the stress $\underline{\sigma}$. The mechanical constitutive equations are therefore expressed as follows:

$$\begin{bmatrix} \dot{\underline{\sigma}}^j = p_0^j \underline{a}^u \dot{\underline{\varepsilon}} - \frac{\underline{\sigma}^j - \underline{\sigma}^{j,r}}{\tau^j} \\ \underline{\sigma}^{j,r} = p_0^j \underline{a}^r \underline{\varepsilon} \\ \dot{\underline{\sigma}} = \sum_{j=1}^N \dot{\underline{\sigma}}^j \end{bmatrix} \quad (12)$$

It is important to mention here that the model (12) is derived from a global statistical analysis of the material system response. The modal stress σ^j does not correspond to particular physical phenomena (no simple physical meaning of usual microplasticity) but represents a statistical averaging quantity of the microstate stress. According to the relaxation spectrum (see FIG. 2), the lowest is the mode, the highest is its contribution to the global response of the material system.

\underline{a}^u et \underline{a}^r are functions of the elastic modulus (E^u, E^r) and the Poisson's ratios (v^u, v^r) for an isotropic material which is the case here. The parameters with superscript u correspond to the unrelaxed regime of the material response involving delay effects. The superscript r corresponds to the relaxed regime where the material responds instantaneously to the external loading, i.e. microstructural variations generated by the external loading without delay. The relaxation time of the j mode is obtained from equations (10) and (11) by:

$$\tau^j = \mu \exp \left(\frac{\Delta F^{j,r}}{RT} \right) \exp \left(\frac{K_\sigma J_2(\underline{\sigma} - \underline{\sigma}^r)}{RT} \right) \quad (13)$$

The expression $K_\sigma J_2(\underline{\sigma} - \underline{\sigma}^r)$ characterizes the variation from equilibrium of the equivalent stress. An exponential evolution of the activation volume parameter with respect to the accumulated inelastic strain $p = \int_0^t J_2 \left[(\underline{a}^u)^{-1} \frac{\underline{\sigma}^j(s) - \underline{\sigma}^{j,r}(s)}{\tau^j(s)} \right] ds$, inspired from the hardening description used in the classical plasticity models [Lemaître and

Chaboche (1985)], has been proposed by the authors [Dieng, Abdul-Latif, Haboussi, and Cunat (2005)]. This formulation pointed out hereafter allows the description of the cyclic softening and hardening phenomena (model 1):

$$K_\sigma = K_{\sigma 0} (1 + A_w \exp(-B_w p)) \quad (14)$$

where $K_{\sigma 0}$ is the initial value of K_σ . A_w and B_w are material parameters controlling the amplitude and the rate of cyclic hardening, respectively.

The mathematical expression of K_σ (equation 14) shows, at least, a limitation concerning the description of the softening phenomenon due to the change in the loading direction after a phase during which an additional hardening is recorded as a result of a biaxial non-proportional loading. For this purpose, a new mathematical definition is proposed in the present paper (model 2):

$$K_\sigma = K_{\sigma 0} [1 + A_w \exp(-B_w p) + H(p - p_0) (1 - \exp(-B_{w2}(p - p_0)))] \quad (15)$$

The Heaviside threshold function, $H(p - p_0)$, is used for the hardening-softening transition phenomenon taking place during the change in cyclic loading direction from complex to simple loading. The evolutions of K_σ versus the accumulated inelastic strain (p) for the two models (1 and 2) are represented in FIG. 3. It is important to keep in mind that this cyclic behavior change can be reproduced by the new model 2 parameters (p_0 and B_{w2}). The parameter p_0 represents a certain value of accumulated inelastic strain after which the softening process occurs. Hence, this parameter can be experimentally measured. Furthermore, the parameter B_{w2} describes the rate of the softening phenomenon.

Finally, the model 2 contains 10 adjustable parameters for an isotropic material (including 2 elastic parameters). Two additional parameters are thus introduced compared to the model proposed by the authors [Dieng, Abdul-Latif, Haboussi, and Cunat (2005)] (noted model 1).

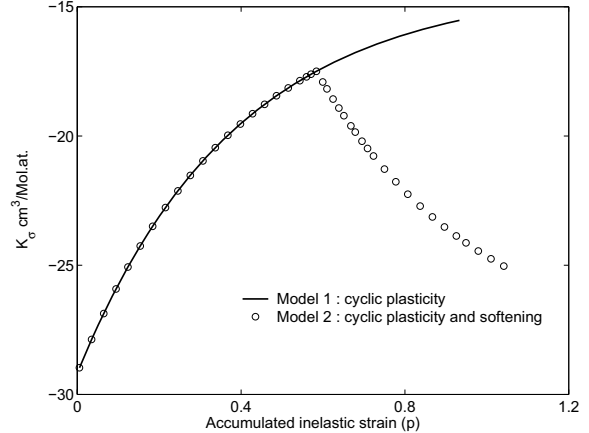


Figure 3: Modification made on the activation volume K_σ to describe the hardening-softening phenomenon

3 Application of the model

3.1 Interpretations of the studied phenomenon

Several researchers studied (for example, Abdul-Latif, Clavel, Ferney, and Saanouni (1994); Ferney, Hautefeuille, and Clavel (1991); Stoltz and Pineau (1978)) the mechanical behavior of Waspaloy (Nickel-based alloy) under proportional and non-proportional cyclic loadings. The size of the precipitates γ' is obtained by two heat treatments, which are: under-aged (UA) and over-aged (OA) states. Indeed, the size of the precipitates, directly influenced by the heat treatment, is of great importance on the mechanical behavior of this alloy as shown in Ferney (1994).

Generally, the mechanical behavior of the UA state can be characterized by shearing process of γ' precipitates. During proportional loading paths, the plastic strain localizes tightly in intense slip bands of the plane {111} and the directions <110> [Abdul-Latif, Clavel, Ferney, and Saanouni (1994); Ferney (1994)]. The activated slip systems are pairs of perfect dislocation types with the absence of twining. Moreover, in-between intense slip bands, very few dislocations are observed [Ferney, Hautefeuille, and Clavel (1991)] in accordance with the localization of the deformation process. Because of small (but numerous) stacking faults scattered in-between bands, there-

fore, the main part of the extra-hardening comes from the isotropic component. According to Ferney (1994), this is due to the interaction between the stacking faults, which exists on different slip systems (latent hardening). It is shown that slip system multiplication enhances isotropic hardening. In this UA state, two microstructural mechanisms take place: the plastic strain localization in the form of slip bands as well as the cyclic softening which follows this strain localization [Pineau (1979)]. These two mechanisms provoke a local degradation of the precipitates. It is worth emphasizing that the repeated shearing phenomenon of the precipitates during cyclic loading is considered as a base to interpret the existence of these two mechanisms [Pineau (1979)]. According to Pineau, the shearing process of precipitates (often orderly) leads probably to the loss of hardening order of the alloy. This explanation has been obviously adopted by Calabrese and Laird (1974). In spite of the wide study performed by Ferney (1994) on this UA Waspaloy, a fundamental question arises concerning the remarkable cyclic hardening: an abrupt decreasing of the isotropic hardening evolution during the first cycles and the softening phenomenon recorded after the steady state in all applied cyclic loading types (simple and complex). Undoubtedly, these physical phenomena are governed by a mechanism (or mechanisms) of the second phase shearing process being coupled with the dislocation motion mechanisms [Abdul-Latif (1996)]. Note that these phenomena cannot be reproduced by the current theoretical development. Hence, their effects can not be taken into consideration during the present identification processes.

Experimentally, an increase of the non-proportionality of the loading path induces a phenomenon of additional hardening. In order to interpret this phenomenon provoked by this non-proportionality, Clavel et al. [Clavel, Pilvin, and Rahouadj (1989)] pointed clearly out that a 90° out of phase angle between tension and torsion strains generates a substantial increase in the number of slip traces in the case of the UA state. According to Ferney et al. [Ferney, Hautefeuille, and Clavel (1991)], an out-of-phase

angle of 90° leads to a multiplication of the number of traces by a factor close to 2. It is now well known that the multiplication of slip systems provokes principally an additional hardening of isotropic nature. On the other hand, the origin of the kinematic hardening of the Waspaloy alloy comes almost from two levels of incompatibility: granular and intergranular. In the current state of knowledge, it proves to be difficult to give a physical interpretation to the intergranular kinematic work hardening. Nevertheless, Ferney (1994) shows that the over-aged state induces a substantial increase in the kinematic part whose origin is primarily intragranular.

3.2 Identification processes

The constitutive equations of the model (Table 1) are programmed into a special computer code: SiDoLo [Pilvin (1995)] in order to calibrate the material constants by using an appropriate experimental database for the UA of Waspaloy [Clavel, Pilvin, and Rahouadj (1989); Ferney (1994)]. Experimentally, the tests have been carried out at room temperature on a servo-hydraulic INSTRON machine (type 1340) using thin-walled tubes (internal diameter: 15.8 mm, external diameter: 18 mm). To identify the model parameters, two cyclic tests are chosen: tension-compression (TC), and out-of-phase tension-torsion, with a sinusoidal waveform, and a phase lag of 90° between the two sinusoidal signals (TT90). The axial and shear strains ($\varepsilon(t)$, $\gamma(t)$) are defined by:

$$\begin{aligned}\varepsilon(t) &= \varepsilon_0 \sin \omega t \\ \gamma(t) &= \gamma_0 \sin(\omega t - \varphi)\end{aligned}\quad (16)$$

with $\frac{\gamma_0}{\varepsilon_0} = \sqrt{3}$; ε_0 and γ_0 are the amplitudes of the axial and shear strains respectively, ω the frequency of an oscillation and φ is the phase angle between the two strains. The maximum von-Mises equivalent plastic strain was maintained constant at 0.5 percent during the test. This gives for uniaxial tension-compression test,

$$\varepsilon_{eq_{max}}^p = \frac{\varepsilon_{max}^p - \varepsilon_{min}^p}{2} = 0.5\% \quad (17)$$

Table 1: Governing equations and parameters of the proposed model 2

Stress evolution
$\begin{cases} \underline{\dot{\sigma}}^j = \underline{a}^u \dot{\varepsilon} p_0^j - \frac{\underline{\sigma}^j - \underline{\sigma}^{j,r}}{\tau^j} \\ \underline{\dot{\sigma}} = \sum_{j=1}^{50} \underline{\dot{\sigma}}^j \end{cases}$
Relaxed stress evolution
$\underline{\dot{\sigma}}^{j,r} = p_0^j \underline{a}^r \dot{\varepsilon} \quad \underline{\dot{\sigma}}^r = \sum_{j=1}^{50} \underline{\dot{\sigma}}^{j,r}$
Relaxation time expression
$\tau^j = \frac{h}{K_B T} \exp \left[\frac{\Delta F^{+,j,r}}{RT} \right] \exp \left[K_\sigma \frac{J_2(\underline{\sigma} - \underline{\sigma}^r)}{RT} \right]$
Non linearity function:
$K_\sigma = K_{\sigma 0} [1 + A_w \exp(-B_w p) + H(p - p_0)(1 - \exp(-B_{w2}(p - p_0)))]$
Accumulated inelastic strain:
$p = \int_0^t J_2 \left[(\underline{a}^u)^{-1} \frac{\underline{\sigma}^j(s) - \underline{\sigma}^{j,r}(s)}{\tau^j(s)} \right] ds$
j mode weight, p_0^j :
$p_0^j = \frac{\sqrt{\tau^{j,r}}}{\sum_j \sqrt{\tau^{j,r}}}$
10 parameters for isotropic material
$\underline{a}^u(E^u, v^u); \underline{a}^r(E^r, v^r); \Delta F_{max}^r; K_{\sigma 0}; A_w; B_w; B_{w2}; p_0.$

and

$$\varepsilon_{eq\max}^p = \max \left(\sqrt{\varepsilon_p^2 + \frac{\gamma_p^2}{3}} \right) = 0.5\% \quad (18)$$

for biaxial tension-torsion test.

In this work, the used databases are related to two types of cyclic loading. In fact, a biaxial tension-torsion test (TT90) with a phase angle (ϕ) equals to 90° being applied up to cyclic steady state. Then, a uniaxial of tension-compression (TC), as second phase, is performed with the same maximum equivalent plastic strain by cancelling the shear strain component. The description of the cyclic behavior of the Waspaloy under such a type of loading sequence (referred to TT90-TC) by the developed model represents the main goal of this work.

Generally, the identification process is a hard task especially in the case of non-linear material behavior. The computer code used to calibrate all the model parameters is based on the resolution technique of the non-linear optimization problem using iterative method to identify these parameters. As in [Dieng, Abdul-Latif, Haboussi, and

Cunat (2005)], to perform this process, several cycles up to stabilization are chosen. The identification process begins by determination of the initial value of the model parameters. These initial parameters should be chosen based on the available experimental results. The following procedures are adopted to appropriately achieve this task: the experimental values of the Young's modulus and the Poisson's ratio ($E = E^u$ instantaneous Young's modulus, $v = v^u$ instantaneous Poisson's ratio) are determined from the first cycle of TC (precisely the first loading in tension) and the Poisson's ratio is initially defined by having an almost standard value of 0.3. The six other parameters are identified by giving for each one an initial value based on a parametric study as well as on the form of the hysteresis loops. The used technique to identify the six other parameters is based on the fact that limiting values (maximum and minimum) are given for each parameter. By fixing all the identified parameters initially calibrated (E^u and v^u), these parameters are thus determined by conducting several iterations. Table (2) summarizes the calibrated coefficients

Table 2: Identified parameters

Parameters	Model 1	Model 2
E^u (MPa)	215000.00	215000.00
ν^u	0.32	0.32
E^r (MPa)	40078.47	21388.12
ν^r	0.495	0.495
ΔF_{max}^r (J/mol.at.)	105246.30	105300.00
$K_{\sigma 0}$ (cm ³ /mol.at.)	-21.99	-20.75
A_w	0.94	0.70
B_w	2.39	5.76
B_{w2}	—	0.89
p_0	—	0.62

of the Waspaloy. Note that the initial values of these coefficients (except the new ones: B_{w2} and p_0) which are used in the identification process, have been already defined by the authors [Dieng, Abdul-Latif, Haboussi, and Cunat (2005)]. The two new model 2 parameters responsible for describing the cyclic softening phenomenon should be calibrated (specially B_{w2}). Actually, an appropriate technique is used to successfully determine the value of both new parameters. In fact, the value of p_0 (as accumulated inelastic strain just before the beginning of the cyclic softening) is experimentally measured. Then, by fixing all other identified parameters, B_{w2} is therefore identified by conducting several iterations and the best results are obtained when the deviation between the experimental and theoretical results becomes minimal (FIG. 4).

3.3 Numerical integration and finite element implementation

Usually, the level of sophistication of the model implemented should be weighed with accuracy and efficiency considerations as well as the qualitative and quantitative knowledge of the material. A fairly accurate representation of the Waspaloy behavior is required to make analysis results meaningful. In the present work, the idea is to assess the validity and the feasibility of the finite element simulation of the cyclic softening phenomenon captured under a complex straining

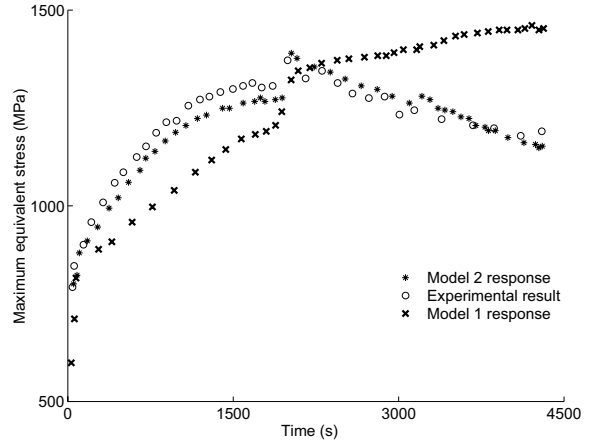


Figure 4: Evolution of the maximum equivalent stress under TT90 loading followed by TC: Comparison between the experimental results and the two models responses

(TT90-TC). In order to carry out structural calculations with the model 2, the related constitutive equations are implemented in a commercial finite element code (Msc Marc/Mentat). Such an implementation is conducted as a local process through the user's subroutine. It is well known that these equations are necessary for each individual finite element integration point of the structure meshing. In this section, the numerical integration of the model is demonstrated and discussed.

The integration of the nonlinear constitutive equations (12) is performed using the simplest way of

the Euler explicit scheme. An incremental approach is programmed and the stress response of the RVE at time $(t + \Delta t)$ is explicitly function of the strain increment.

For the model constitutive equations, the material point response represents the sum of N contributions for different modes. From a numerical point of view, to successfully capture the contribution of one mode j , the used time increment should be lower than the corresponding relaxation time. In this case, the CPU time may be very expensive for a general calculation due to the size of the lowest relaxation time (3 hours for a tensile test for one material point on a ultra 5 Sun computer). It has been fortunately remarked [Dieng (2002)] that the modes with weak relaxation times have a considerably slight effect on the overall response (less than 0.5%) due to their weights. In the light of this fact, the CPU time problem is therefore overcome by neglecting the latter contribution during the calculation process.

3.4 Numerical simulation of a thin-walled tube

The mechanical behavior of the Waspaloy at room temperature is numerically studied in this section. As given above, all experiments are carried at room temperature using thin-walled tubes (internal diameter: 15.8 mm, external diameter: 18 mm, see FIG. 5-a). Since the structure behavior can not be axisymmetric with respect to TT90-TC test, all the elasto-plastically deformed zone (weakest zone) made from the Waspaloy is thus modeled (see, FIG. 5-b). The specimen is subdivided into 144 elements with a 8 nodes cubic element. It is rigidly fixed (cantilever) at one of its extremities, while the second extremity is cyclically loaded with an axial and tangent displacements having a sinusoidal form with 90° out-of-phase angle between the two displacements. This leads consequently to the fact that each of the extremity section nodes is submitted to such a loading path. The application of this loading path provokes three types of shear, one is planar and the others are transversal. The transversal ones perturb slightly the simulated response in (x,y) plane due to the coupling effect generated by the equivalent stress in the shift function ($\exp\left(\frac{K_\sigma J_2(\underline{\sigma} - \underline{\sigma}')}{RT}\right)$)

involved in equation (13). The numerical evolution of the maximum equivalent cyclic Mises stress during cycling prediction is compared with both experimental and model 2 results as shown in FIG. 6. It is noticeable now that the structural calculation shows a successful description of the cyclic plasticity behavior of the Waspaloy, notably the cyclic softening phenomenon.

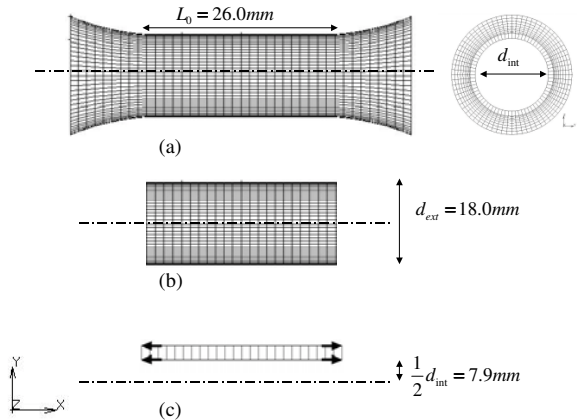


Figure 5: Finite Element specimens

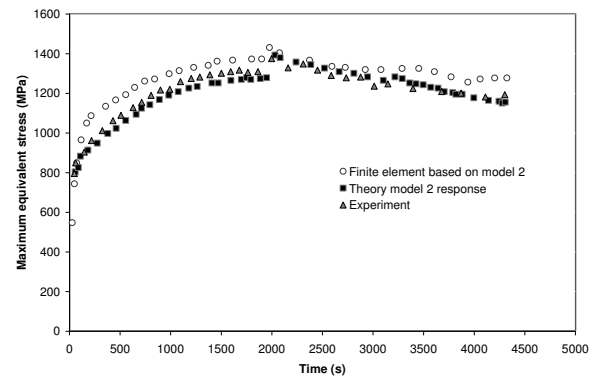


Figure 6: Evolution of the maximum equivalent stress under TT90 loading followed by TC: Comparison between the experimental result, finite element and the model 2 responses

4 Remarks and Conclusion

Let us discuss now the different quantitative applications conducted in this work. After programming the two models (1 and 2) and identifying their related parameters, some issues should be

now discussed in order to demonstrate the capability of the new extension to describe not only the classical cyclic plasticity phenomena but also the more complicated one (i.e., cyclic softening).

It is well known that the cross hardening effect appears when a proportional cyclic straining in a given direction is replaced, after stabilization, by another proportional one having different direction (for example, Benallal and Marquis (1987); Krempl and Lu (1984)). Hence, the change in the loading direction, with the same equivalent strain range, leads to a strengthening during the transition between the two loading sequences followed by a progressive softening. However, in our case, the non-proportional cyclic straining (TT90) is applied up to steady state and then followed by a uniaxial (TC) one with the same maximum equivalent plastic strain. According to FIG. 4, the same phenomenon is recorded for the Waspaloy, i.e., an abrupt strengthening followed by a slow softening. This strengthening is almost due to the cross hardening effect. On the other hand, the softening phenomenon is interpreted by the fact that a partial decrease in the number of slip traces takes place giving an intermediate value, ranging between that of TC test (having the minimum value) and the maximum value observed during TT90 test [Clavel, Pilvin, and Rahouadj (1989)].

By consulting the identified parameters of both models 1 and 2, the first remark reveals the fact that several important differences are well recorded during the actual identification especially for the model parameters E^r and B_w . In fact, such differences can be interpreted as follows. Because of the new parameters p_0 and B_{w2} (in reality, only one (B_{w2}) which needs identification using the special software as the other (p_0) is measured), the calibration of all other model parameters (except E^u and v^u) are conditioned by the new ones and should be obtained by a best fit between the theoretical and experimental results. Moreover, according to the high sensitivity of the model to the parameter (ΔF_{max}^r) as shown in [Dieng, Abdul-Latif, Haboussi, and Cunat (2005)], the relatively small change in its value leads consequently to these changes in the other mentioned parameters. Despite the difference between the

values of the two models parameters, one can clearly notice that they have almost equivalent responses as shown in related figures of this work.

As far as the comparisons between the models and experiments are concerned, FIG. 4 shows a comparison between the experimental results and the predictions of the two models 1 and 2. For this material, in the first phase, an out-of-phase angle of 90° provokes an additional hardening mainly of an isotropic nature. In this phase, the two models can describe this hardening evolution. In fact, the first model describes somewhat reasonably this additional hardening due to those parameters already identified in [Dieng, Abdul-Latif, Haboussi, and Cunat (2005)]. However, the model 2 describes in a more accurate manner this phase. By canceling the shear strain component (second phase of this loading path), a cross hardening effect and a subsequent cyclic softening take place. Once again, it is clear that the model 1 finds rapidly its limitation in reproducing the softening phenomenon, while the model 2 with the new extension predicts it correctly. This is undoubtedly governed by the new proposed equation (15) in which the parameter K_σ , strongly related to the activation volume i.e. the atomic mobility, represents a fundamental key to answer this problem as pointed clearly out in FIG. 3. Moreover, the correlated solutions of the two models are evidently in good agreement with the experimental results under uniaxial cyclic loading (TC) (FIG. 7) as well as under biaxial cyclic loading (TT90) (FIG. 8). FIG. 6 confirms that the obtained numerical predictions by finite element method show its successful ability to reproduce the metallic structure behavior under such complex cyclic phenomenon.

As final conclusions, these models (1 and 2) describe successfully the uniaxial and biaxial cyclic behaviors of the Waspaloy at room temperature. However, in order to predict a more complicated phenomenon, i.e., the cyclic softening, it is clear now that without the new extension of the DNLR model, such a phenomenon cannot be represented. It is important to underline that model 2 is always able to suitably reproduce other cyclic plasticity features for the same material. Once

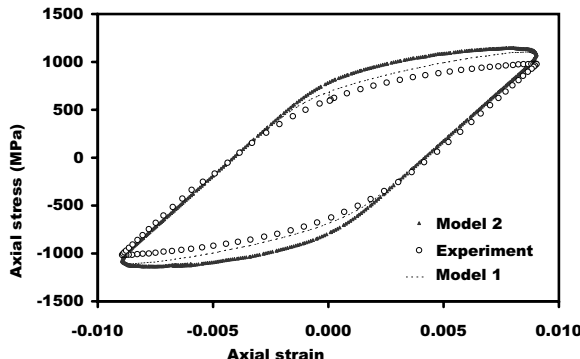


Figure 7: Evolution of the tensile stress under a TC loading: Comparison between the experimental results and the two models responses

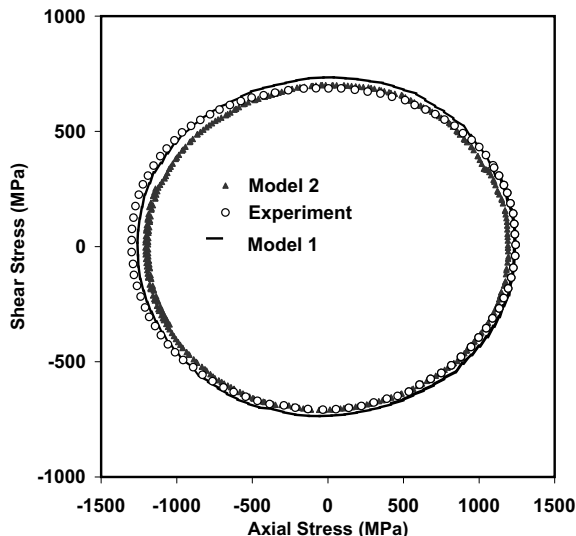


Figure 8: Stress responses under loading (TT90): Comparison between the experimental results and the two models responses

more, the implementation of the new extension of the DNLR model in the commercial finite element code is appropriately performed. The obtained numerical predictions by finite element method predict fairly well the experiments.

References

- Abdul-Latif, A.** (1996): Constitutive Equations for Cyclic Plasticity of Waspaloy. *Int. J. Plasticity*, vol. 12, pp. 967–985.
- Abdul-Latif, A.; Clavel, M.; Ferney, V.; Sa-**
- nouni, K.** (1994): On the Modeling of Nonproportional Cyclic Plasticity of Waspaloy. *ASME J. Engng. Mater. Techn.*, vol. 116, pp. 35–44.
- Benallal, A.; Marquis, D.** (1987): Constitutive Equations for Nonproportional Cyclic Elasto-Viscoplasticity. *ASME, J. Engng. Mater. Techn.*, vol. 109, pp. 326–336.
- Blackmon, D. R.; Socie, D. F.; Leckie, F. A.** (1983): Application of Continuum Damage Concepts to Creep-Fatigue Interactions. *ASME Symp. on Thermal and Environmental Effects on Fatigue*, vol. 109, pp. 45–57.
- Calabrese, C.; Laird, C.** (1974): Cyclic Stress-Strain Response of Two-Phase Alloys - Part II, Particles not Penetrated by Dislocations. *Mater. Sci. Eng.*, vol. 13, pp. 159–175.
- Clavel, M.; Pilvin, P.; Rahouadj, R.** (1989): Analyse Microstructurale de la Déformation Plastique Sous Sollicitations Non Proportionnelles dans un Alliage Base Nickel. *Comptes Rendus de l'Académie des Sciences*, vol. 309, pp. 689–696.
- Cunat, C.** (2001): The DNLR Approach and Relaxation Phenomena. Part I - Historical account and DNLR formalism. *Mechanics of Time Dependent Materials*, vol. 5, pp. 39–65.
- DeDonder, T.** (1920): *Leçons de Thermodynamique et de Chimie Physique*. Gauthier-Villars, Paris.
- Dieng, L.** (2002): Sur un Modèle de Comportement Mécanique avec Analyse Modale de la Dissipation: Mise en Oeuvre et Validation Numériques. Technical report, Thèse de Doctorat, I.N.P. Lorraine, 2002.
- Dieng, L.; Abdul-Latif, A.; Haboussi, M.; Cunat, C.** (2005): Cyclic Plasticity Modeling with the Distribution of Non-Linear Relaxations (DNLR) Approach. *Int. J. Plasticity*, vol. 21, pp. 353–379.
- Dieng, L.; Haboussi, M.; Loukil, M.; Cunat, C.** (2005): Theory of Inelasticity Based on a Non-equilibrium Thermodynamic: Application to yield surface prediction. *Mechanics of Materials*, vol. 37, pp. 1069–1081.

- Doong, S. H.; Socie, D. F.** (1991): Constitutive Modeling of Metals under Nonproportional Cyclic Loading. *ASME J. Engng. Mater. Techn.*, vol. 113, pp. 23–30.
- Eyring, H.** (1936): Viscosity, Plasticity and Diffusion as Examples of Absolute Reaction Rates. *J. Chem. Phys.*, vol. 4, pp. 283–287.
- Fatemi, A.; Kurath, P.** (1988): Multiaxial Fatigue Life Prediction under the Influence of Mean-Stresses. *ASME J. Engng. Mater. Techn.*, vol. 110, pp. 380–388.
- Ferney, V.** (1994): Etude de l'Ecrouissage Cyclique sous Sollicitations Complexes. Technical report, Thèse de Doctorat, Université de Technologie de Compiègne, 1994.
- Ferney, V.; Hautefeuille, L.; Clavel, M.** (1991): Influence de la Microstructure sur l'Ecrouissage Cyclique d'Alliages à Durcissement Structural en Sollicitations Multiaxiales -Partie II. *Mémoires et Etudes Scientifiques Revue de Métallurgie*, vol. 7-8, pp. 679–689.
- Gibbs, G. B.** (1970): Thermodynamic Systems for Analysis of Dislocation Glide. *Phil Mag*, vol. 22, pp. 701–706.
- Kanazawa, K.; Miller, K. J.; Brown, M. W.** (1977): Low Cycle Fatigue under Out-of-Phase Loading Condition. *ASME J. Engng. Mater. Techn.*, vol. 99, pp. 222–228.
- Krempl, E.; Lu, H.** (1984): The Hardening and Rate dependent Behavior of Fully Annealed AISI Type 304 Stainless Steel under Biaxial in Phase and Out-of-Phase Strain Cyclic at room Temperature. *ASME J. Eng. Mater. Techn.*, vol. 106, pp. 376–382.
- Lamba, H. S.; Siddebottom, O. M.** (1978a): Proportional Biaxial Cyclic Hardening of Annealed Oxygen-Free High-Conductivity Copper. *Journal of testing and Evaluation*, vol. 106, pp. 206–267.
- Lamba, H. S.; Siddebottom, O. M.** (1978b): Cyclic Plasticity for Non-proportional Paths. *ASME J. Eng. Mat. Techn.*, vol. 100, pp. 96–111.
- Lemaître, J.; Chaboche, J. L.** (1985): *Mécanique des matériaux solides*. Dunod, Paris.
- Loukil, M.** (1996): Modélisation des Surfaces de Plasticité à Partir d'une Approche de le Thermodynamique de la Relaxation des Milieux Continus. Technical report, Thèse de Doctorat, I.N.P. Lorraine, 1996.
- McDowell, D. L.** (1985): An Experimental Study of the Structure of Constitutive Equations for Nonproportional Cyclic Plasticity. *ASME J. Eng. Mater. Techn.*, vol. 107, pp. 307–315.
- Meixner, J.** (1949): Thermodynamik und Relaxationerscheinungen. *Z. Naturforschung*, vol. 4a, pp. 494–600.
- Pilvin, P.** (1995): Manuel d'Utilisation du Logiciel SiDoLo. Technical Report Version 2.3, 1995.
- Pineau, A.** (1979): Sollicitation Cyclique des Alliages Durcis par Précipitation, Dislocations et Déformation Plastique. *Yravals Les Editions de Physique*, pp. 383–393.
- Poynting, J. H.; Thomson, J.** (1902): *Properties of Matter*. Griffin and Co., London.
- Prigogine, I.** (1968): *Introduction à la Thermodynamique des Processus Irréversibles*. Dunod, Paris.
- Stoltz, R. E.; Pineau, A. G.** (1978): Dislocation-Precipitate Interaction and Cyclic Stress-Strain Behavior of a γ' Strengthened Superalloy. *Mat. Sci. Eng.*, vol. 34, pp. 275–284.

